Low Frequency GFRP Imaging with Variable Aperture TFM

Philippe Rioux[1], Renato Nogueira[2], Sam Hughes[3],
[1,] Sonatest, Québec, Canada
[1]Phone: (418) 683-6222x117, e-mail: philippe.rioux@sonatest.com
[2]e-mail: renato.nogueira@sonatest.com
[3]e-mail: sam.hughes@sonatest.com

ABSTRACT

Graphite or glass fibre reinforced polymer (GFRP) inspections are usually made with a zero-degree linear scan (L-scan). The Total Focusing Method may not be applicable for some anisotropic materials, but TFM may increase the ultrasound imaging quality in some cases. The imaging potential of 1D linear probes has been broadened by TFM in many aspects, so there is an opportunity to apply the total focusing concepts to exotic composite assessment. The ultrasonic limitations associated with testing thicker sections of GFRP restrict inspections to lower frequency phased array probes. When using the L-Scan technique, a low-frequency probe will have a poorer sensitivity performance once compared to a typical phased array probe of a higher frequency. This is due to the element size and pitch restrictions associated with low-frequency probes. Therefore, new testing techniques should be found. The alternative imaging acquisition method involves variable aperture receivers that improve the typical L-Scan characteristics. This study explicitly covers the differences between the L-scan type, the TFM image and its variable aperture TFM feature. In addition to the theory concepts, ultrasound metrics have been recorded on an actual GFRP sample.

Keyword: TFM improvements, Composite Inspections, Total Focusing Method (TFM), GFRP, Aperture, Phased Array Ultrasonic Testing (PAUT), Glass Fibre, Concrete

INTRODUCTION

Challenge

An existing 3-meter (10-foot) outside diameter concrete/GFRP pipeline in Texas is due for a maintenance inspection. The challenge consists of evaluating the integrity of its 70 mm (2.75 inches) nominal thickness. The primary customer requirements only needed a thickness evaluation and lamination detection, providing the best information the current techniques allow. The probe frequency will consequently limit the size of the smallest defect. The compromise is caused by a large grain anisotropic GFRP material structure. The probe choice should allow the detection of anything above 1.75 mm (wavelength/4) and will not likely scatter on its fibre size less than 0.7 mm (wavelength/10^{i}). The advantage of this 0.5 MHz probe is the low attenuation response over thick composite material. Our material has a much larger attenuation coefficient than 100 dB/m for a 5 MHz probe which places the part far from the 1-10 dB/m amplitude drop for usual steel and aluminum properties. Typically, a PA probe's frequency range is within 2.25 to 7.5 MHz, but the specifications of the 0.5MHz model offer a different range of properties. A few metrics are shown in the following table:

X3A Probe	X6B Probe	Ratio Difference
0.6 mm pitch	2 mm pitch	3.33x
38.4 mm active aperture	128 mm active aperture	Idem
5 MHz	0.5 MHz	10x
0.7 mm wavelength	7 mm wavelength	Idem

Table 1 Probe Specifications Comparison

Linear Scan Testing

Zero-degree inspections are generally solved by a linear scan (L-scan) that uses a sequence of small (usually about eight) virtual aperture shots that finally creates a side image underneath the probe.

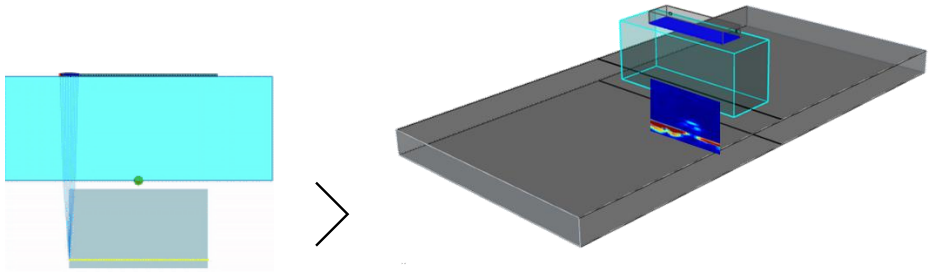

Figure 1 L-scan Sketch

TFM Testing

Using the same equipment (Instrument, probe and wedge), it is possible to generate a TFM image designed for linear applications. The TFM scan uses the LL Propagation Mode calibrated at 3500 m/s for the compression wave mode. For the acquisition step, many different receiving aperture sizes have been tested. The default TFM ordinarily uses 100% of the Rx elements. In other words, this represents 64 sequences of one Tx element for all 64 (100%) Rx elements.

The smaller captured matrix may contain a sparse matrix capture (SMC) parameter of 6%, 12%, 25%, 50% and 100%. The dark grey cells can be wider as the Rx aperture is also nearer to 100%. In contrast to full FMC, the SMC created less refracted-angle elementary A-scans. The smallest RX size created only near zero-degree refracted angles.

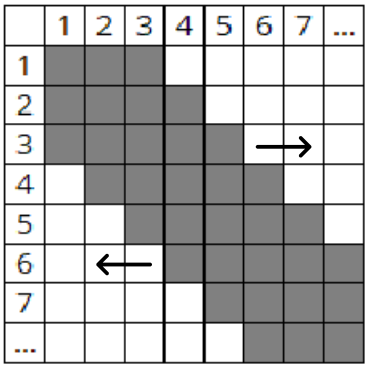

Figure 2 Example of a 2 Rx Element Matrix on Each Side of 1 Tx Element

For example, the eight-element SMC setting has a 24-degree coverage, and the full 64-element TFM is 84 degrees open. The near zero-degree LL legs are more powerful than high-angle components, and that makes an optimised imaging mapping technique.

This scanning pattern is very close to the dynamic depth focus (DDF) method. On the other hand, the DDF method is designed to fire and receive a symmetrical aperture, while TFM always uses 1 transmitting element in this study.

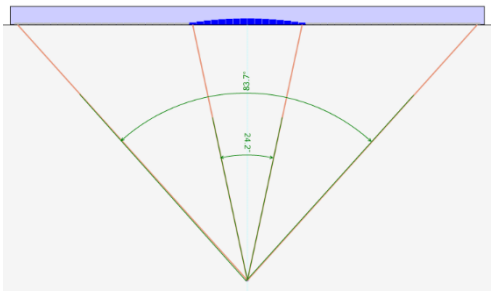

Figure 3 Angle Focus Limit Lines for a 16-Element TFM vs. Its Full Aperture

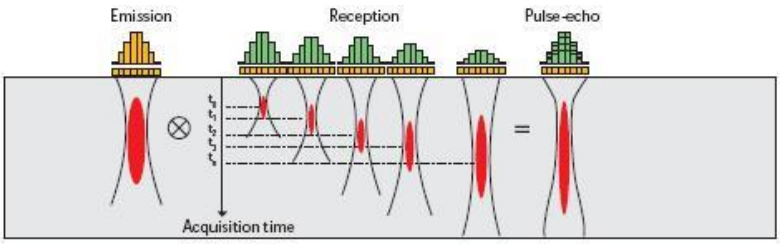

Figure 2 Illustrated DDF Acquisition[ii]

This SMC/TFM technique considerably increases the frame rate acquisition speed because it requires fewer elementary A-scans to process and less pulse and receives signals. By having similar and known advantages to DDF, this unique TFM acquisition should decrease all the constant focusing disadvantages of a zero-degree linear scan. It is worth noting that TFM LL legs may also contain higher refracted angle components than DDF.

Material Properties

There are many types of GFRP. The sample used for this study is a blend of the composite and concrete technique. The following weight ratio has been described in the chemical content datasheet:

- Between 15 and 50% of polyester resin or vinyl ester
- Between 0 and 50% of crystalline silica sand and/or calcium carbonate (Chalk)
- Between 5 and 30 % of fibreglass
  express

We compared the GFRP sample properties to an existing velocity study about GFRP.[iii] Our part has a density of 2.24 g/cm^3 and a velocity of 3500 m/s at 0.5 MHz at 22 degrees Celsius. They confirmed the effect of higher velocity on low proportions of epoxy/resin glue. The current testing sample contains a very high quantity of fibreglass but also a high ratio of minerals. The sand and chalk densities are higher than fibreglass, which also explains the high density. The sound velocity is closer to the concrete property, which is about 3500 and 4000 m/s. [iv]

Figure 3 Material Cut out Section

Methodology

Three side drilled holes (SDHs) have been made on the sample to allow more tests. All SDHs are 1.9 mm in diameter. TCG points could then be recorded at 25%, 50% and 75% of their nominal thickness. These reflectors were also used to evaluate the beam width dimension, signal-to-noise ratio and attenuation.

A VEO3 32:128 instrument with Full Matric Capture (FMC) and TFM recording capabilities was used as the data acquisition system. The probe is an X6B-0.5M64E-2x10-SQX5. The couplant is water by direct contact inspection.

Signal to Noise Ratio

This test requires two measurements, the baseline noise amplitude in front of the reflector (SDH in this case) and the amplitude of the SDH. The ratio is expressed in dB by the following formula.

$$SNR(dB) = 20 * Log(\frac{\%\ FSH\ Baseline\ Noise}{\%\ FSH\ Reflector})$$

Beam Width

This dimension is parallel to the active aperture index axis. The beam width ends at 6 dB lower than its centerline highest amplitude.
The beam error is half the TFM resolution and half the pitch for the L-scan. (±0.25 mm and ±1 mm, respectively)

RESULTS

SNR Comparison

We fixed the L-scan aperture and delays, and we compared the SNR on three different focusing depths. The minimum acceptable SNR is determined at 6 dB (i.e. a factor of two between a reflector and noise)[v]. When the reflectors were inside the focal range, only the 22 and 32-element aperture L-scans passed the SNR criterion.
There is, although, a major limitation when using high aperture focusing on fixed element delay sequences. Figure 5 is an example of the 32-element side view when the focusing is close to the SDH and when the focusing depth is 35 mm away from it. The SDH size is too large when the focus is offset by its location. On top of that, the SNR fails as well.

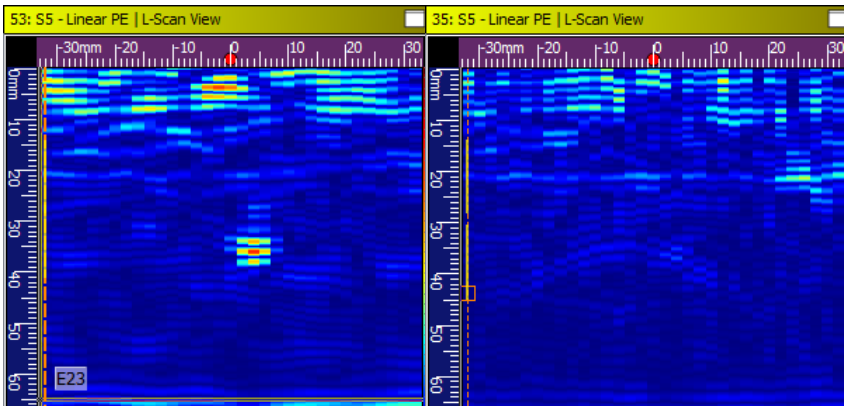

Figure 4 SDH Inside the Focal Range (left) and SDH Outside of the Focal Range (right)

L-scan & TFM SNR Performance

The number of active elements for both acquisition types makes a difference for the receiving energy. This is also affecting both the SNR and the required scanning gain. The following graph displays the SNR performance regarding the number of elements used in the scan.

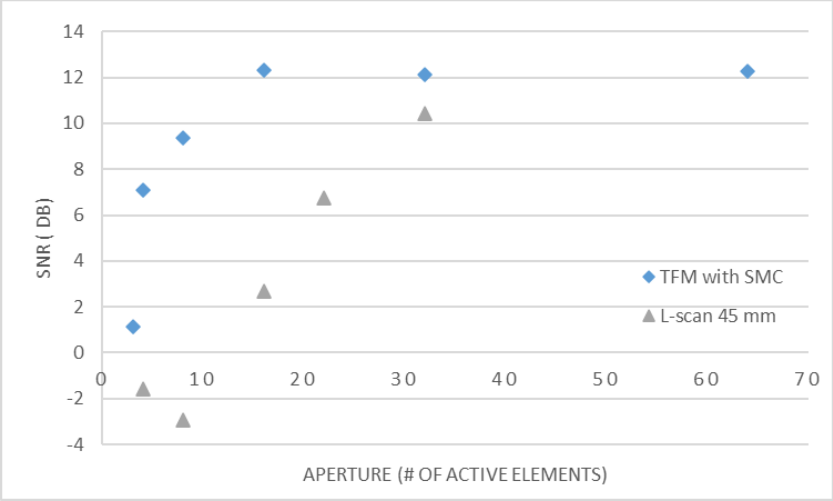

Figure 5 SNR on TFM and L-scan (higher is better)

It is also interesting the see the required scanning gain for the two techniques. The predicted gain behaviour was a higher scanning gain inspection for lower aperture size sequences.

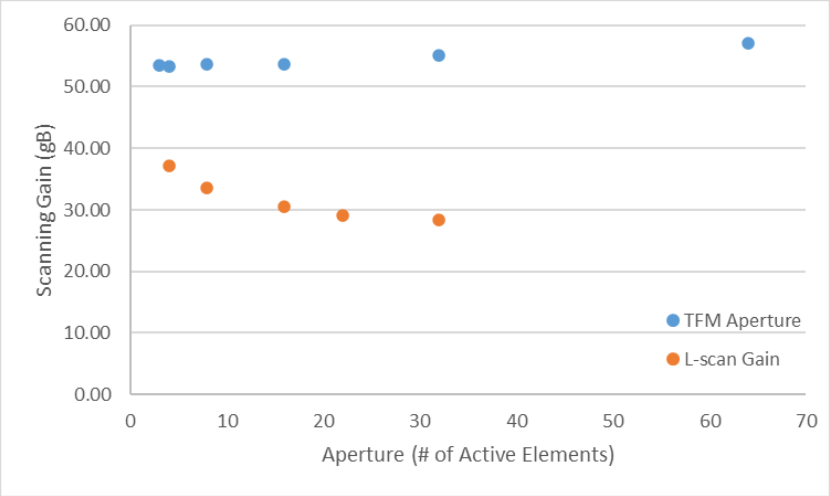

Figure 6 Scanning Gain Compared to Different Apertures (lower is better)

The TFM passes using a 4-element Rx SMC, while the L-scan must have 22 elements or more active aperture to be acceptable. As the TFM is always focused on each pixel, the amplitude response is continually optimised for inside the nominal thickness. The 16-element TFM SMC is by far the most interesting SNR compromise. The noise floor remains the same, giving out a 10 dB (3.1x) better ratio. The 16 Rx element aperture TFM SNR is 12 dB, while its sister L-scan SNR is as low as 2 dB.

Together with the SNR, Figure 7 provides a comparative result over the amplitude sensitivity for the same reflector. We can compare the gain over different aperture sizes thanks to the normalized A-scan amplitude feature. Otherwise, the 16-element versus the 32-element scan would appear 6 dB better (twice the element, 2x more sensitive). The TFM requires about 12 more dB than the L-scan, but the 55 dB scanning gain is only at two-thirds of the entire instrument gain range. The maximum acquisition gain is 80dB.

SDH Echo Width Comparison

The inspection must respect the SNR essential criteria, although its echo width result may also affect the sizing performance. The large, fixed aperture L-scan focusing is likely to cause a narrow beam despite its short focal range. The SDH echo spot is weak and wide, as confirmed in the situation in Figure 5 on the right. An unfocussed 32-element beam width gives the worst sizing among all the tests. Still, this is the best accuracy dimension when the echo is inside its focal range. Figure 8 includes each available scan type's dynamic SDH envelope dimensions.

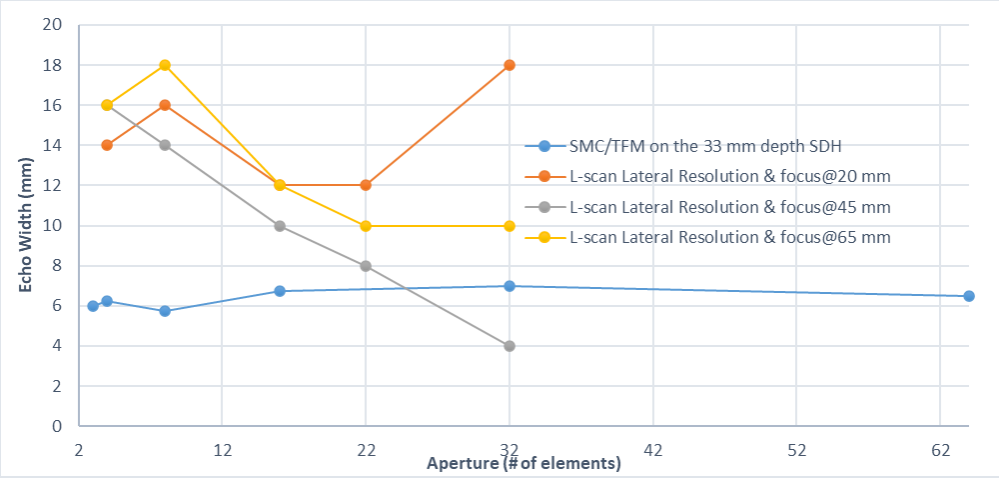

Figure 7 Echo Width of One SDH Result over TFM and L-scan Active Aperture

The TFM provides a constant and low beam width effect for all apertures and reflector positions. This is the most critical and compelling performance compared to traditional L-scans. Even the small Rx TFM aperture data is showing consistent results. Please note that sample SDH is 1.9 mm in diameter, and the probe wavelength is 7 mm. This is a ratio of 27%, and the sensitivity response is acceptable. The 6 mm echo width is very close to the wavelength, but there is no relationship between the two. The wavelength dimension axis effect is perpendicular to the horizontal echo width.

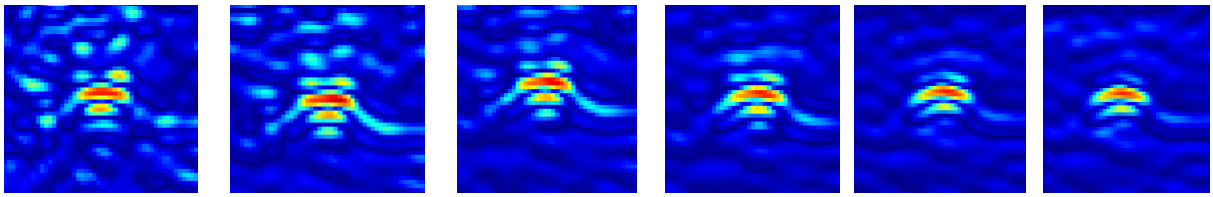

Figure 8 Left: Smallest Aperture TFM; Right: Full 64E Aperture

TCG Results

Timed-Corrected Gain (TCG) is useful when that material attenuation makes it difficult to size assessment over great distances. There is a preferred area where TCG amplification can be repetitively applied. We recorded the amplitude dynamic echo along the index axis from 3 different depths. This way, we could compare the BeamTool sensitivity map and check where the calibration TCG zone limit ends. Figure 10 is an example of one dynamic echo along the active aperture (right half only). The BeamTool10 sensitivity result over a larger region of interest (ROI) than the probe index length.

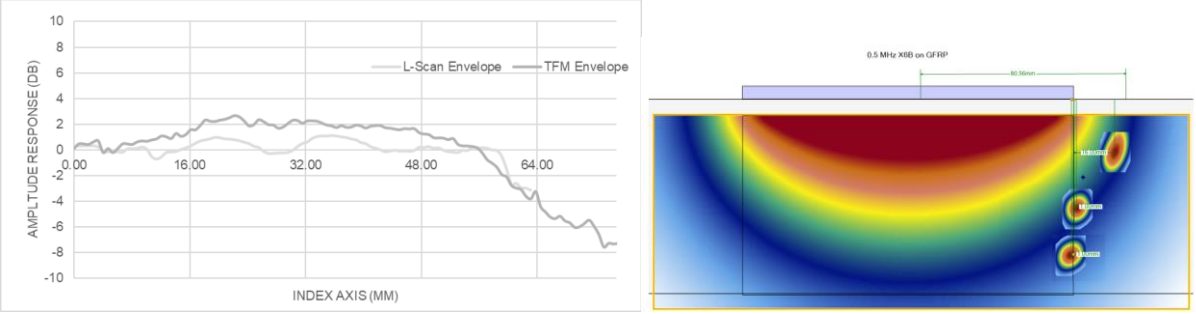

Figure 9 Dynamic SDH Envelope and BeamTool 10 Sensitivity Simulation

As the ROI can be larger than its probe equivalent L-scan index width, the amplitude dramatically drops outside the element's zero-degree area. When the SDH reflector reached down to 20 %, the first 17 mm depth TCG point could be set as far as 16 mm away from the probe. The middle and deepest SDH reflector could only be calibrated at the end of the last element. According to the TCG point data, the 4 Rx element aperture TFM only requires an overall 1 dB more gain than a 16 Rx element TFM.

We could extract a 0.21 dB/mm amplitude drop along the 45 mm SDH constant depth line once the ROI is outside the element index zone. The average TCG vertical line compensation has been estimated at 0.125 dB/mm. (125 dB/m or 3.175 dB/inch)

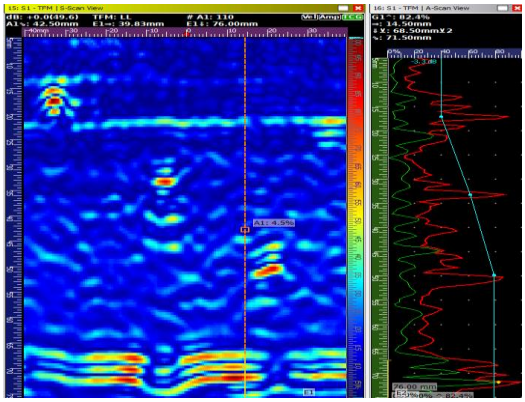

Figure 10 TCG Image Result and Its Red Dynamic Envelope on the Right

CONCLUSIONS

This low-frequency inspection could never be solved entirely without the TFM capabilities. The L-scan could not pass based on low SNR results. Even the high aperture sequences reveal a short focal range, hence very short ROI. The TFM and small aperture SMC is a good compromise that alleviates all L-scan issues. TFM is also interesting for larger ROI inspection and higher lateral resolution. For practical TCG purposes, calibrating underneath the probe's active area is easily performed and recommended.

This imagery method additionally confirms its better beam width performance, providing better sizing accuracy. This recent imaging technique could be applied for most existing L-scan applications, such as corrosion mapping. This TFM recording process could even be applied on a wide 128-element PA probe using the existing instrument without the entire 128:128 pulse and receive power.

REFERENCES

[i] Krautkramer, Herbert.Grabendorfer, W. (Werner). Ultrasonic testing. Springer-Verlag Berlin Heidelberg GmbH 1990 p.115

[ii] https://www.ndt.net/ndtaz/content.php?id=693 the NDT Encyclopedia, Ed Ginzel.

[iii] Wrobel, G. and Pawlak S. "The effect of fiber content on the ultrasonic wave velocity in glass/polyester composites" 2007. Journal of achievements of materials and manufacturing engineering.

[iv] Ni Nyoman Kencanawati, Akmaluddin1, Buan Anshari, Ahmad Gazi Paedulla2, and Mitsuhiro Shigeishi. "The study of ultrasonic pulse velocity on plain and reinforced damaged concrete". MATEC Web of Conferences 195, 2018 p.6

[v] ISO/DIS 22232-3:2018, Non-destructive testing — Characterization and verification of ultrasonic test equipment — Part 3: Combined equipment. Section 6.5 and Section 6.5.3 p.7